

## NEW 145-MHZ SOURCE MEASUREMENTS BY PAPER IN THE SOUTHERN SKY

DANIEL C. JACOBS<sup>1,2</sup>, JAMES E. AGUIRRE<sup>1</sup>, AARON R. PARSONS<sup>3</sup>, JONATHAN C. POBER<sup>3</sup>, RICHARD F. BRADLEY<sup>4,5,6</sup>, CHRIS L. CARILLI<sup>7</sup>, NICOLE E. GUGLIUCCI<sup>6</sup>, JASON R. MANLEY<sup>8</sup>, CAREL VAN DER MERWE<sup>8</sup>, DAVID F. MOORE<sup>1</sup>, CHAITALI R. PARASHARE<sup>4</sup>

*Accepted by ApJ Letters: 6 May 2011*

### ABSTRACT

We present observations from the Precision Array for Probing the Epoch of Reionization (PAPER) in South Africa, observed in May and September 2010. Using two nights of drift scanning with PAPER's 60° FWHM beam we have made a map covering the entire sky below +10 degrees declination with an effective center frequency of 145 MHz, a 70-MHz bandwidth, and a resolution of 26'. A 4800 square-degree region of this large map with the lowest Galactic emission reaches an RMS of 0.7 Jy. We establish an absolute flux scale using sources from the 160-MHz Culgoora catalog. Using the 408-MHz Molonglo Reference Catalog (MRC) as a finding survey, we identify counterparts to 480 sources in our maps, and compare our fluxes to the MRC and to 332 sources in the Culgoora catalog. For both catalogs, the ratio of PAPER to catalog flux averages to 1, with a standard deviation of 50%. This measured variation is consistent with comparisons between independent catalogs observed at different bands. The PAPER data represent new 145-MHz flux measurements for a large number of sources in the band expected to encompass cosmic reionization, and represents a significant step toward establishing a model for removing foregrounds to the reionization signal.

*Subject headings:* dark ages, reionization, first stars — catalogs — instrumentation: interferometers

### 1. INTRODUCTION

Emission from the highly redshifted 21 cm line of neutral hydrogen is a very promising method of exploring the Epoch of Reionization (EoR) over the redshift range  $6 < z < 12$  (Furlanetto, Oh, & Briggs 2006; Fan, Carilli, & Keating 2006). Several EoR experiments are currently operating, including the Murchison Widefield Array (MWA; Lonsdale et al. 2009), the Low Frequency Array (LOFAR; Röttgering et al. 2006) the Giant Metre-wave Radio Telescope (GMRT; Paciga et al. 2011), and the Precision Array for Probing the Epoch of Reionization (PAPER; Parsons et al. 2010). Both PAPER and the MWA operate in the southern hemisphere, as will the future Square Kilometer Array (SKA). It is anticipated that to effectively suppress foreground emission many orders of magnitude brighter than the EoR signal, these instruments will need high levels of observational stability and exquisite characterization and control of instrumental systematics. These goals will be greatly aided by building a complete sky model that includes accurate point-source locations and fluxes.

Several recent attempts have been made to synthesize what is known about the radio sky from existing surveys. de Oliveira-Costa et al. (2008) compiles measurements from 10 MHz to 90 GHz and uses them to create a global sky model of extended emission (sizes greater than two degrees). Discrete sources are listed in many catalogs.

Those used for comparison here are listed in Table 1.

The literature grows increasingly sparse at lower frequencies and in the southern hemisphere; indeed, *no* blind survey has been reported below 408 MHz in the south. The SPECFIND cross-identification catalog identifies 6000 unique sources between 100 and 200 MHz with  $\delta > 0^\circ$ , but fewer than 1000 sources with declination  $\delta < 0^\circ$ . The best information in the south ( $\delta < -30^\circ$ ) below 408 MHz is provided by the Molonglo 4 Jy Survey (MS4; Burgess & Hunstead 2006), which uses the MRC (complete to 1 Jy), Culgoora observations by Slee (1995) at 160 MHz and 80 MHz, and new Molonglo observations at 408 and 800 MHz to estimate the 178-MHz flux of bright sources in a sample similar to the northern 3CRR survey (Laing, Riley, & Longair 1983).

Catalog comparisons are hindered both by spectral/temporal variation of sources and by differences in the angular resolution of observations. Point-source confusion is of particular concern, given the large synthesized beams of many low-frequency instruments. Spectra at low frequencies tend to be dominated by synchrotron emission. While this emission tends to be well-described by a power-law in frequency, at lower frequencies, several effects complicate comparisons between bands. Chief among these is synchrotron self-absorption, which is most often in evidence at the lowest frequencies, but may also produce spectral features between 100 and 200 MHz (Helmholtz et al. 2008). Another complication arises from sources not present in the deep high-frequency catalogs appearing at lower frequencies due to exceptionally steep spectral indices. A source steep enough to appear in these first PAPER images ( $> 10 Jy$ ) and be absent in the MRC sample ( $> 1 Jy$ ) would need a very steep spectral index  $< -2.2$ . Out of over 70000 sources in NVSS only two or three sources are known to have spectral indices this steep (van Weeren et al. 2009). For these rea-

<sup>1</sup> Dept of Physics and Astron. U. of Pennsylvania, Philadelphia, PA

<sup>2</sup> Corresponding Author: jacobsda@sas.upenn.edu

<sup>3</sup> Astron. Dept., U. California, Berkeley, CA

<sup>4</sup> Dept. of Electrical and Computer Eng., U. Virginia, Charlottesville, VA

<sup>5</sup> Natl. Radio Astron. Obs., Charlottesville, VA

<sup>6</sup> Astronomy Dept., U. Virginia, Charlottesville, VA

<sup>7</sup> Natl. Radio Astron. Obs., Socorro, NM

<sup>8</sup> Karoo Array Telescope, Capetown, South Africa

sons, it is desirable to have measurements in the band of interest at an appropriate resolution.

In this Letter, we present new flux measurements of 480 sources at 145 MHz using PAPER. These measurements cover the largest area of the southern sky yet surveyed in the EoR band. We describe PAPER and the observations in §2, detail our method for calibration and counterpart identification in §3 and conclude in §4 with prospects for future improvements.

## 2. OBSERVATIONS AND DATA REDUCTION

PAPER is a first-generation experiment focusing on the statistical detection of the fluctuations in HI emission during the EoR. It is an interferometric transit array operating between 110 and 180 MHz ( $7 < z < 12$  for HI). PAPER consists of two deployments: a 32-antenna array at the NRAO facilities near Green Bank, WV, and a 32-antenna array in South Africa’s Radio Quiet Zone (PAPER South Africa, hereafter PSA32). The final PSA instrument will consist of 128 full-Stokes dipole antennas. The data presented here are from the initial deployment of PSA32.

Each PAPER antenna is a pair of crossed sleeve dipoles mounted above a mesh ground screen. Signals from each antenna are amplified, directly digitized, and then correlated by an FPGA-based correlator (Parsons 2008). PAPER’s primary beam is  $60^\circ$  FWHM with a spatially- and spectrally-smooth response nearly to the horizon. A point at zenith takes about 4 hours to cross PAPER’s primary beam, during which time apparent flux changes by a factor of two.

The PSA32 antennas are arranged in a minimum redundancy configuration, constructed to provide uniform sampling of the  $uv$ -plane within a 300-meter-wide circle while avoiding a central radius of 10 m (Parsons et al. 2011). The maximum baseline length of this arrangement generates an effective resolution of  $26'$  at 145 MHz. Antenna positions were surveyed using a commercial differential GPS to centimeter precision. We found no further position refinement necessary.

During May and September 2010, we recorded commissioning data with PSA32 in two separate campaigns. Between the May and September data-taking, a number of small improvements to the correlator were made, but all other hardware remained unchanged. The data presented here are from UT 2010 May 19 13:11 - 2010 May 20 04:50 (15 hours) and UT 2010 Sep 15 16:48 - 2010 Sep 16 04:04 (12 hours), both periods being predominantly between sunset and sunrise. Only the linear EW dipoles of each antenna were correlated. Visibilities were integrated and recorded every 5.37 seconds. The frequency resolution was 96 kHz in May and 45 kHz in September. The separation in LST between the two observing epochs, along with PAPER’s wide primary beam, make these two observations sufficient to map the entire sky below  $\delta < 10^\circ$ .

Data editing, calibration and imaging were performed using the Astronomical Interferometry in PYthon (AIPY) package<sup>9</sup>. The first analysis step was to obtain a phase calibration. Because of the wide field-of-view (FOV) of the antennas, the data are dominated by bright sources that are sometimes far from the zenith. Dur-

ing the May observation, the brightest source visible was Cen A<sup>10</sup>, while the brightest source during September observations was Pic A. These sources are bright enough to perform single-baseline fringe fitting. Data observed within ten minutes of the transit of these sources were used to derive a phase calibration by fitting a time and frequency visibility model to the data using a conjugate-gradient solver (Parsons et al. 2010). Phase terms in the calibration are dominated by cable and correlator delays; these have been found to be quite stable. Thus for the analysis here, the phase calibration derived from these two 10-minute observations is applied to each night’s entire observation.

If the source is not carefully removed, the phase-calibrator sidelobes severely limit imaging dynamic range. An efficient source-removal technique filters data by removing the corresponding region of delay/delay-rate (DDR) space for each baseline (Parsons & Backer 2009). This technique filters a source from each baseline by nulling data having a delay and fringe-rate corresponding to the desired sky location.

The net effect is to remove a large fraction of the filtered source *without* having to construct a multi-source image-domain model. For the May data, the point-source component of Cen A (estimated flux  $\sim 5000$  Jy) is filtered; for September, we have removed Pic A and For A (400 and 150 Jys, respectively).

Given the high quality of the RFI environment at the Karoo site, RFI-flagging was limited to flagging of a few satellite bands, as well as any visibilities with amplitudes  $2\sigma$  above the mean amplitude as in Parsons et al. (2010). Less than one percent of the data are flagged in this way.

In this quiet environment, instrumental effects became dominant. A troublesome instrumental effect in many interferometric instruments is common-mode interference, interfering signals common to two or more inputs and sky signals crossing antenna boundaries within the analog system. Both of these kinds of cross-talk are removed by subtracting a 4 hour long running average as described in Parsons et al. (2010).

Map-making is done in three stages: snapshot-imaging, mosaicking each night and finally summing into a single calibrated map.

Images are made in 10-minute zenith-phased “snapshots”; this is a sufficiently short time that the effects sources moving through the primary beam is negligible. Visibility data are gridded into the  $uv$ -plane using linear multi-frequency synthesis (Taylor, Carilli, & Perley 1999) and  $w$ -projection (Cornwell, Golap, & Bhatnagar 2008). To this  $uv$ -gridded data we apply radial weighting—increasing radially in the  $uv$ -plane—to emphasize point sources. Gridded data are Fourier transformed to produce a snapshot image  $70^\circ$  wide, with an effective synthesized beam width of  $26'$ . These facets are then deconvolved by the equivalent dirty beam using the Högbom CLEAN algorithm (Högbom 1974). Image-domain deconvolution is limited in its ability to reconstruct the flux, particularly in the wide-field case (Rau et al. 2009). Thus, the CLEANing is not fully effective, and the images contain artifacts from the side-lobes of sources far from the phase center.

<sup>10</sup> While Cen A is resolved, the central point source dominates the smooth structure by several orders of magnitude.

<sup>9</sup> <http://casper.berkeley.edu/astrobaki/index.php/AIPY>

All snapshot images made over the course of a night are weighted by a model of the primary beam and averaged onto a HEALPIX grid (Górski et al. 2005) with  $7'$  pixels ( $\text{NSIDE}=512$ ), to create two maps — one for each epoch. A typical pixel has weighted contributions from approximately five snapshots. Each map is flux-calibrated to a bright source near the phase-calibrator using a flux taken from the Culgoora catalog. The May map is flux-calibrated to 1422-297 at 21 Jy and the September map is calibrated to 0521-365 at 72 Jy. Once on the same flux-scale, the two epoch maps are summed together into a single map, weighted by the number of snapshot contributions. The final product covers 36000 square degrees at  $\delta < 10^\circ$ , with an effective resolution of  $26'$ .

The limitations of these reduction steps, as well as instrumental artifacts, impact image fidelity. Final images include residual cross-talk and errors due to delay-filtering, which necessarily removes flux from multiple points on the map. The absence of time-dependent calibration, the limitation to image-plane deconvolution and uncertainty in the beam model also affect the accuracy of the map.

Successful future work in foreground mapping and EoR detection will depend on our ability to correctly identify the most important of these issues. This is true not only within the PAPER project, but also between similar projects. For these reasons we establish an accuracy baseline by measuring and comparing the fluxes of many sources to catalog values.

### 3. CATALOG CONSTRUCTION AND FLUX CALIBRATION

We have used the entire sky below  $\delta < 10^\circ$  to find fluxes corresponding to 480 MRC sources above 4 Jy — selection criteria similar to those used by Burgess & Hunstead (2006) to generate the MS4 sample. The PAPER flux is identified as the brightest pixel within  $30'$  of the MRC source. They are listed along with separation distances and local RMS in Table 2; 90% of the sources identified are within one beam-width (see Figure 3). In the following we will explore the relative completeness and accuracy of this catalog.

The accuracy of the PAPER image and of these fluxes can be evaluated both superficially in the image plane and numerically by comparing to past measurements. By comparing the MRC catalog directly to the image we can ascertain the relative completeness of the MRC sample. In Figure 1 we overlay MRC markers from our 4-Jy subsample onto a 4800 square-degree sub-image and see that at the 4-Jy flux-level MRC is not one-to-one but does agree with the map on all but one source. As shown in Figure 2 this source manifests a rare high-frequency turn-over.

In the case of the Culgoora catalog, there are no such differences. In places where Culgoora shows a bright source that is not in the 408 MHz sample, PAPER also finds a bright source. Sources as dim as 10 Jy do not have a matching MRC marker. Together these facts suggest that by limiting to MRC sources above 4 Jy we have excluded sources with steep ( $\alpha < -1$ , where  $S = S_0(\frac{\nu}{\nu_0})^\alpha$ ) spectra. These steeper sources are below our flux limit at 408 MHz but are bright at 145 MHz. Thus our complete flux-limited sample of MRC at 408 MHz becomes incomplete at 145 MHz.

To assess the accuracy of the flux measurements we

compare with 332 sources also found in the Culgoora catalog and 225 found in MS4. The accuracy of the PAPER measurements will be limited by the image dynamic range, as discussed above, as well as the relatively wide bandwidth of the PAPER. However these errors must be set against the error in the catalog comparison. As can be seen in the Helmboldt or SPECFIND collections of radio spectra, the presence of multiple components or extended structure in sources hampers comparisons between observations with different resolutions, while the presence of self-absorption or other spectral structure impedes comparison between catalogs generated at different frequencies. To set the scale of these effects we intercompare several catalogs with measurements near the PAPER band.

A simple comparison metric is the per-source flux-scale; the ratio of fluxes between two sets. Accounting for spectral slope, the flux-scale would have a nominal value of one, with a certain amount spread encompassing all the sources of error in flux determination and catalog comparison. In Figure 3 we have plotted the distributions for the PAPER/Culgoora and PAPER/MRC<sup>11</sup>. To estimate the catalog comparison error we have calculated the MRC/Culgoora flux-scale, as well as between all sources in SPECFIND at 151-MHz and those at 178-MHz. The SPECFIND comparison has the advantage of more accurate cross-identification between sources. In addition, most of the measurements in these bands were done by the Cambridge Low Frequency Telescope (6 and 7C) and the 3CR all of which are known to be in good agreement (Bennett 1962; Gower, Scott, & Wills 1967; Baldwin et al. 1985). Even so, a noticeable (although narrower) spread of flux scales is apparent (Figure 3). In the SPECFIND comparison 90% of sources are below a flux-scale of 1.5, while in all other comparisons the 90% level occurs at 1.75. The distribution of the MRC/Culgoora flux comparison has a spread similar to the distribution of PAPER's fluxes relative to each of these catalogs.

The MRC sources have been cross-identified with the Culgoora using the same algorithm as the MRC-PAPER cross-identification. Thus the MRC-Culgoora comparison would be more likely to have similar catalog comparison errors and in fact does have a similar distribution of flux-scales. This similarity implies that systematic errors will not be easily distinguished by catalog comparison. As an example consider the most extreme flux-scale outlier 0123-016 (3c40). PAPER observes a flux of 26 Jy while Culgoora only 8.9 Jy. Culgoora notes this source to have multiple components and measures 32 Jy in the 80-MHz band. When we add 3C and 3CR to the spectrum we see a consistent picture of a source around 30 Jy as shown in Figure 2 with the 160-MHz point the only in disagreement. Catalog discrepancies of *this* type are rare but there are many types.

### 4. DISCUSSION AND CONCLUSIONS

The Epoch of Reionization signal will be faint; detection will require precise calibration as well as deep

<sup>11</sup> Where fluxes were measured at frequencies outside of the PAPER band (110-180 MHz), we have scaled the flux using a spectral index of  $\alpha = -1$  (the average index at these frequencies; Slee 1995; Helmboldt et al. 2008; Bennett 1962)

foreground removal. Self-calibration of a wide-field instrument requires knowledge of sources covering a large fraction of the sky. This calibration may then be verified by comparing multiple measurements, ideally between telescopes.

To facilitate such comparison, we publish here the first catalog derived from early PAPER data which, despite suffering from various systematics related to instrument response and analysis methodology, shows qualitatively good agreement with other measurements. Our demonstrated ability to map more than half of the sky with two days of observation represents a major advance in survey speed and is made possible by the width of PAPER's primary beam, the bandwidth of PAPER's correlator, and the use of w-projection.

A number of improvements to the instrument and data processing methodology are currently underway. Cross-talk can be mitigated by the addition of one-way RF coupling and Walsh switching. Both are likely to reduce excess correlations though their effectiveness are still being evaluated.

Preliminary work is also under-way to refine imaging using the Common Astronomy Software Applications (CASA) environment<sup>12</sup>. Early tests of Cotton CLEAN, faceting combined with w-projection, time-dependent calibration, and spectroscopic imaging have been favorable; this system will be used to produce higher dynamic range maps suitable for a blind survey and spectroscopic exploration. Finally, the dynamic range is limited

by the instantaneous  $uv$ -coverage of the 32-element antenna configuration. Future deployments with larger number of antennas will result in additional improvements to the snapshot  $uv$ -coverage and imaging dynamic range.

Implementing these instrumentation and processing improvements will help produce images of even higher fidelity that might reach the sub-Jy confusion limit. From such images, it will be possible to construct a complete blind catalog using source fitting and photometric analysis. This more precise catalog will merit a stricter comparison with previous catalogs that more carefully accounts for extended structure and confusion.

Compared to the current array, the final PAPER South Africa array will have four times as many elements and should have 16 times the dynamic range. Here we have imaged and cataloged what is essentially a dirty image of the sky and already found good agreement. The final PAPER telescope will be capable of spectral imaging the 110 to 180-MHz night sky to the confusion limit once a day. Although the radio sky was first explored at meter wavelengths, much remains unknown about the spectral and temporal behaviour of sources in this frequency band. These early PAPER 32-element commissioning data are already demonstrating a reliable level of accu-

racy that are limited primarily by well-known problems. We can reasonably expect future PAPER data to add substantially to our understanding of the sky at meter wavelengths.

This work made use of the Topcat package<sup>13</sup> as well as the Vizier Virtual Observatory database<sup>14</sup>. AP would like to acknowledge support through the NSF AAPF program (#0901961) and from the Charles H. Townes Postdoctoral Fellowship. The PAPER project is supported through the NSF-AST program (#0804508).

## REFERENCES

- Baldwin, J. E., Boysen, R. C., Hales, S. E. G., Jennings, J. E., Waggett, P. C., Warner, P. J., & Wilson, D. M. A. 1985, *MNRAS*, 217, 717
- Bennett, A. S. 1962, *MNRAS*, 125, 75
- Burgess, A. M. & Hunstead, R. W. 2006, *AJ*, 131, 100
- Cohen, A. S., Lane, W. M., Cotton, W. D., Kassim, N. E., Lazio, T. J. W., Perley, R. A., Condon, J. J., & Erickson, W. C. 2007, *AJ*, 134, 1245
- Condon, J. J., Cotton, W. D., Greisen, E. W., Yin, Q. F., Perley, R. A., Taylor, G. B., & Broderick, J. J. 1998, *AJ*, 115, 1693
- Cornwell, T. J., Golap, K., & Bhatnagar, S. 2008, *IEEE Journal of Selected Topics in Signal Processing*, 2, 647
- de Oliveira-Costa, A., Tegmark, M., Gaensler, B. M., Jonas, J., Landecker, T. L., & Reich, P. 2008, *MNRAS*, 388, 247
- Fan, X., Carilli, C. L., & Keating, B. 2006, *ARA&A*, 44, 415
- Furlanetto, S. R., Oh, S. P., & Briggs, F. H. 2006, *Phys. Rep.*, 433, 181
- Górski, K. M., Hivon, E., Banday, A. J., Wandelt, B. D., Hansen, F. K., Reinecke, M., & Bartelmann, M. 2005, *ApJ*, 622, 759
- Gower, J. F. R., Scott, P. F., & Wills, D. 1967, *MNRAS*, 71, 49
- Helmboldt, J. F., Kassim, N. E., Cohen, A. S., Lane, W. M., & Lazio, T. J. 2008, *ApJS*, 174, 313
- Högbom, J. A. 1974, *A&AS*, 15, 417
- Laing, R. A., Riley, J. M., & Longair, M. S. 1983, *MNRAS*, 204, 151
- Large, M. I., Mills, B. Y., Little, A. G., Crawford, D. F., & Sutton, J. M. 1981, *MNRAS*, 194, 693
- Lonsdale, C. J. et al. 2009, *IEEE Proceedings*, 97, 1497
- Paciga, G. et al. 2011, *MNRAS*, 244
- Parsons, A. e. 2008, *PASP*, 120, 1207
- Parsons, A. R. & Backer, D. C. 2009, *AJ*, 138, 219
- Parsons, A. R. et al. 2010, *AJ*, 139, 1468
- Parsons, A. R., McQuinn, M. and Jacobs, D. C., Aguirre, J., & Pober, J. 2011, *ApJ*, submitted, arxiv:astro-ph/1103.2135
- Rau, U., Bhatnagar, S., Voronkov, M. A., & Cornwell, T. J. 2009, *IEEE Proceedings*, 97, 1472
- Röttgering, H. J. A., Braun, R., Barthel, P. D., van Haarlem, M. P., Miley, G. K., et al. 2006, In *Proc. Cosmol., Galaxy Form. Astropart. Phys. Pathw.* SKA, Oxford, April 1012, 2006. Published by ASTRON (astro-ph/0610596)
- Slee, O. B. 1995, *Australian Journal of Physics*, 48, 143
- Taylor, G. B., Carilli, C. L., & Perley, R. A., eds. 1999, *ASP Conf. Ser.*, Vol. 180, *Synthesis Imaging in Radio Astronomy II*
- van Weeren, R. J., Röttgering, H. J. A., Brügggen, M., & Cohen, A. 2009, *A&A*, 508, 75
- Vollmer, B. et al. 2010, *A&A*, 511, A53+

<sup>12</sup> <http://casa.nrao.edu/>

<sup>13</sup> <http://www.starlink.ac.uk/topcat/>

<sup>14</sup> <http://vizier.u-strasbg.fr/viz-bin/VizieR>

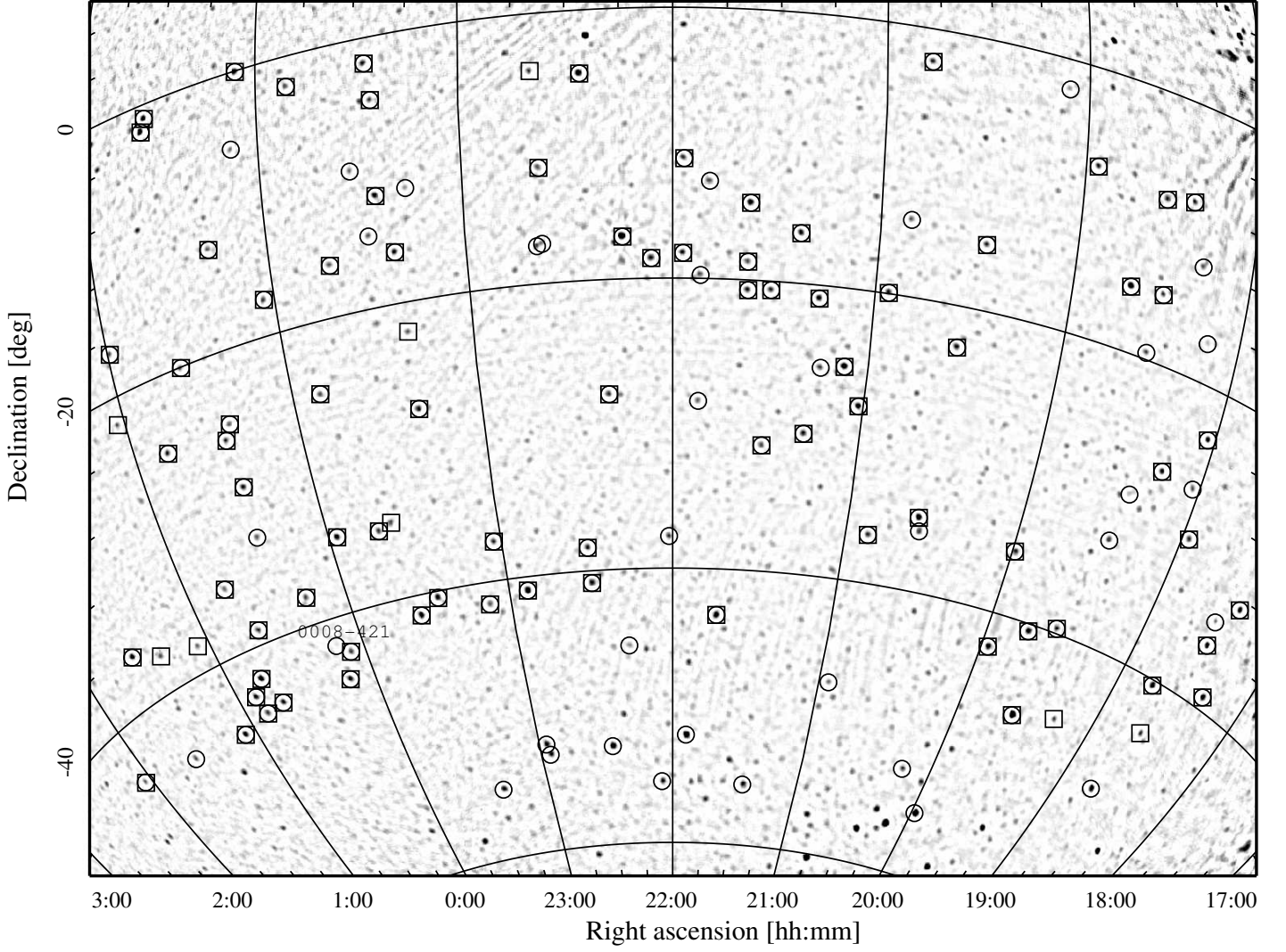


**Figure 1.** A low foreground region of the PSA32 field, centered at  $23^{\text{h}} -31^{\circ}$ . Pixels above 99% of the flux scale, approximately 1 Jy, are shown in black. MRC sources above 4 Jy are shown in circles. PAPER fluxes for these sources are given in Table 2. All MRC markers, save one, have a corresponding source at this flux level. The 160MHz Culgoora survey, used to evaluate the flux scale, is shown in squares. This image has an effective integration time of 30 minutes, a bandwidth of 70MHz, a field rms of 0.4 Jy, and a peak to field dynamic range of 120.

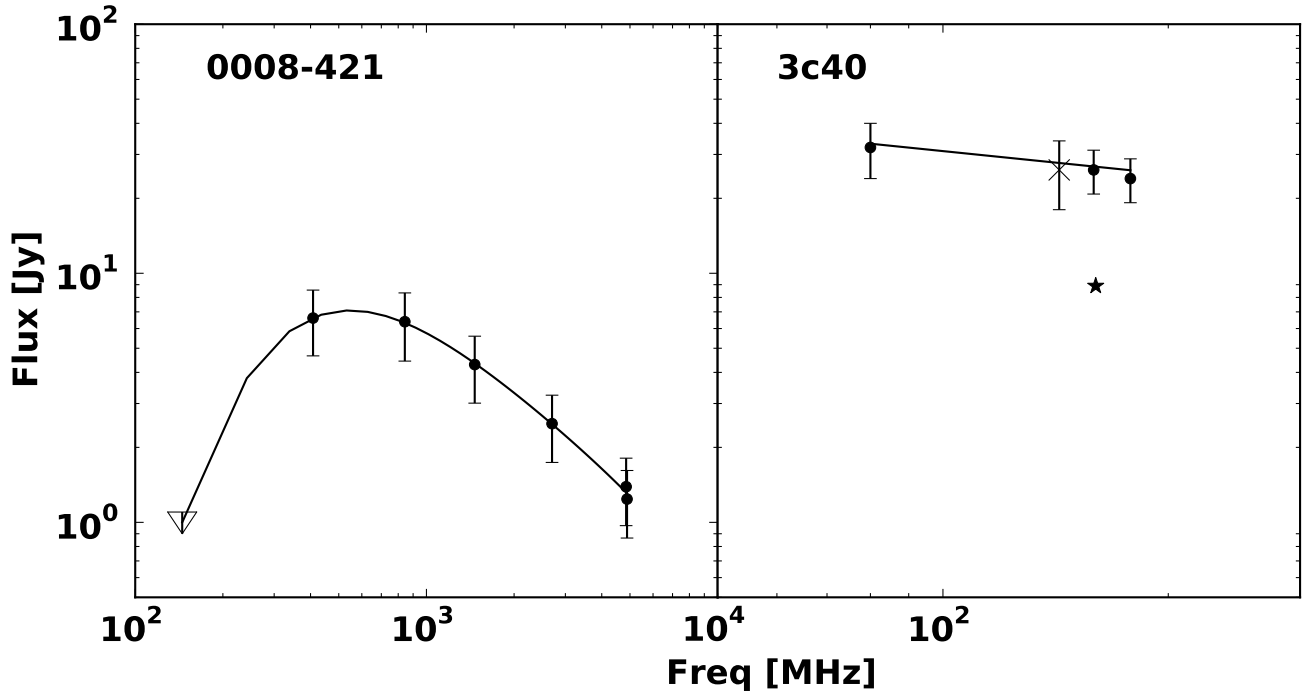


**Figure 2.** Left: Spectrum of 0008-421, the only MRC source in Figure 1 without a PAPER counterpart. A rare example of spectral turnover at around 500 MHz. Right: Spectrum of 3c40 (0123-016) with an 'x' for PAPER flux and star for Culgoora 160-MHz. All circles taken from SPECFIND.

**Table 1**  
Low frequency surveys used in this Letter

Name	Res	Freq [Mhz]	Dec Limits	Flux Limit [Jy]	Ref
MRC	2'	408	$18.5 > d > -85$	1	Large et al. (1981)
MS4	2'	178 <sup>b</sup> , 408	$-30 > d > -85$	4	Burgess & Hunstead (2006)
Culgoora	1.85', 3.7'	160, 80	$32 > d > -50$	2	Slee (1995)
3CR(R) <sup>a</sup>	6'	178	$75 > d > -50$	5	Bennett (1962)(Laing et al. 1983)
6C <sup>a</sup>	4.2'	151	$> 30$	0.3	Baldwin et al. (1985)
7C <sup>a</sup>	1.17'	151	$> 26$	0.2	Gower et al. (1967)
VLSS <sup>a</sup>	80"	74	$> -30$	0.4	Cohen et al. (2007)
NVSS <sup>a</sup>	45"	1400	$> -40$	2.5e-3	Condon et al. (1998)
PAPER	26'	145	$10 >$	10	This Letter

<sup>a</sup> Sources included via the SPECFIND meta-catalog (Vollmer et al. 2010) .

<sup>b</sup> 178MHz fluxes in MS4 are estimates based on MRC, Culgoora and other measurements.

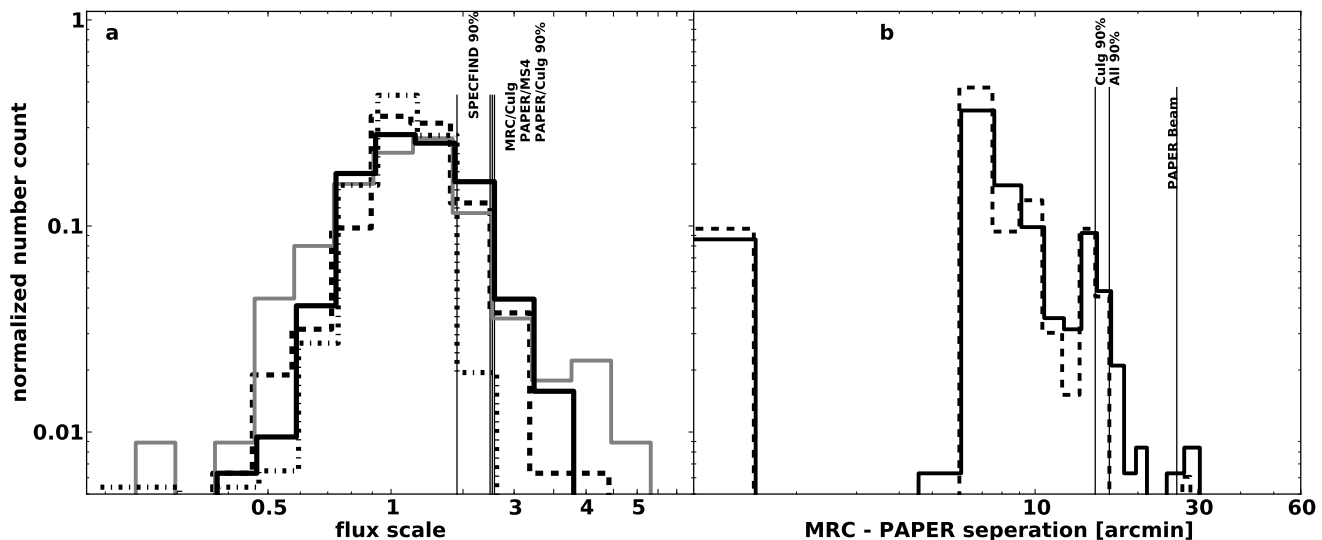


**Figure 3.** a) PAPER’s flux scale —the ratio of PAPER fluxes to Culgoora fluxes at 160MHz (black, solid) and to MS4 fluxes interpolated to 178MHz (grey, solid). PAPER/Culgoora and PAPER/MS4 with FWHM of 1 and 0.7 have distributions similar to the MRC/Culgoora flux ratio (thick, dashed) with a FWHMs of 0.5. A similar comparison between 178 and 151 MHz objects co-identified by SPECFIND (dot-dashed) shows that a somewhat tighter agreement (0.5 FWHM with fewer large outliers) is possible if cross-matching is done while accounting for morphology and instrumentation. b) Distance in degrees between MRC position and identified PAPER peak. All MRC sources within  $-85^\circ < \delta < 10^\circ$  have been paired with a PAPER peak within the plotted range. PAPER positions are defined by the centers of HEALpix pixels that are  $7'$  on a side leading to quantization effects; 90% of sources are within one PAPER beam (thin solid vertical line).

**Table 2**  
PAPER fluxes for 480 MRC sources and matching Culgoora fluxes (where available)

Ra	Dec	Name	S145	rms	MRC_sep	Cul	S(160)	S(80)	SpIndex
0.60	-83.14	0003-833	18.9	4.7	0.17				
0.88	-17.50	0000-177	11.6	1.2	0.11	0000-177	11.8	22	-0.9
1.37	-56.54	0003-567	12.0	2.2	0.17				
1.52	-42.61	0003-428	9.6	1.3	0.16	0003-428	11.9	11	0.11
1.58	-0.07	0003-003	25.5	2.6	0.12	0003-003	16.8	27	-0.68
2.11	-6.05	0005-062	11.2	1.8	0.23	0005-062	6.9	10	-0.54
2.51	-44.50	0007-446	14.3	1.2	0.16	0007-446	17.0	26	-0.61
3.27	-42.11	0008-421	1.5	1.4	0.41				

**Note.** — PAPER Southern Sky catalog generated by searching for sources in the Molonglo Reference Catalog above 4 Jy and below  $+10^\circ$  Declination. Beginning on the left, the columns list: Right Ascension and Declination in degrees, MRC name, calibrated PAPER flux [Jy], rms around source [Jy] and angular separation in degrees from MRC location. Included for reference are Culgoora 160MHz, 80MHz and spectral indices fluxes where available. Complete table available in the online edition these Letters.